

Simple replication methods for producing nanoslits in thermoplastics and the transport dynamics of double-stranded DNA through these slits

Rattikan Chantiwas,^{a,b,e} Mateusz L. Hupert,^{a,b} Swathi R. Pullagurla,^a Subramanian Balamurugan,^a Jesús Tamarit-López,^f Sunggook Park,^c Proyag Datta,^d Jost Goettert,^d Yoon-Kyoung Cho,^e and Steven A. Soper^{a,b,c,e*}

^a Department of Chemistry, ^b Center for Bio-Modular Multi-Scale Systems,

^c Department of Mechanical Engineering, ^d Center for Advanced Microstructures and Devices,

Louisiana State University, Baton Rouge, LA 70803, USA

^e School of Nano-Biotechnology and Chemical Engineering, Ulsan National

Institute of Science and Technology, Ulsan, Korea

^f Departamento de Química, Instituto de Reconocimiento Molecular y Desarrollo Tecnológico,

Universidad Politécnica de Valencia, Camino de Vera s/n, 46071 Valencia, Spain

*Corresponding Author

Email: chsope@lsu.edu, phone: +1 (225) 578-1527, Fax: +1 (225) 578-3458

Investigation of nanoimprinting conditions for nanoslit arrays

For the two-step replication process reported herein, the nanoimprinting conditions (pressure, P_i , and temperature, T_i) were optimized to achieve high replication fidelity and at the same time, minimize deformation of the existing microchannels formed in the previous replication step. The results of the optimization process are presented in Fig. S1. The deformation percentage in this case was defined as the change in the microchannel cross-sectional area following nanoimprinting with respect to the cross-sectional area before imprinting.

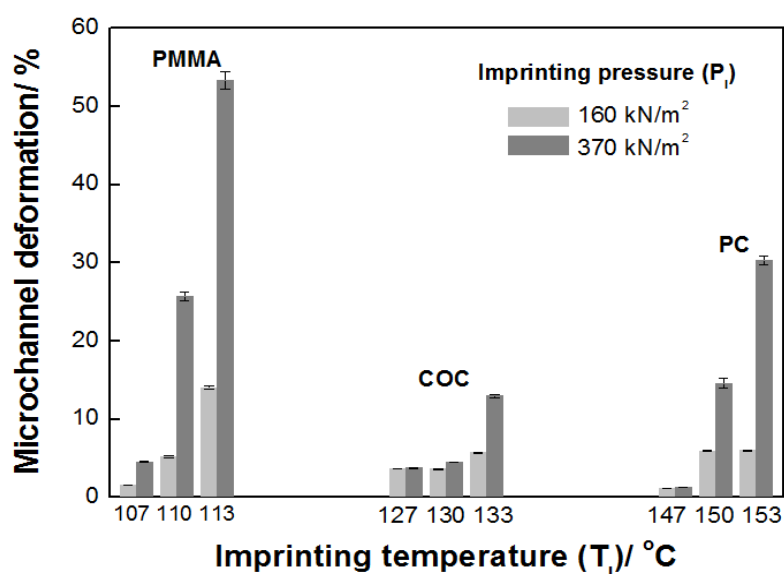


Fig. S1. Deformations in microchannels hot embossed into thermoplastics (PMMA, COC and PC) induced by the subsequent nanoimprinting of the nanoslit arrays. The deformation percentage is shown as a function of the nanoimprinting pressure and temperature. Deformation was expressed as the change in the microchannel cross-sectional area after imprinting to that before imprinting. Error bars represent the standard deviations for at least three measurements on four different microchannels. The T_g of the native thermoplastic materials, PMMA, COC and PC, are 105°C, 134°C and 150°C, respectively.

AFM profiles after chip assembly

Fig. S2 shows AFM profiles of the PMMA and COC nanoslits and the cover plates after chip assembly after they were subjected to oxygen plasma treatment and low temperature thermal fusion bonding (see Table 1 for conditions). The substrates subjected to oxygen plasma treatment

and low temperature thermal fusion bonding showed ~6% (PMMA) and 9% (COC) reduction in the depth of the nanoslits compared to the nanoslits not subjected to thermal processing (see Fig. 4). The cover plate surface profiles (see Fig. S2) showed some sagging of the polymer plate into the nanoslit; the profiles showed features that were 12 (± 2) nm tall for PMMA and 13 (± 2) nm tall for COC with a width matching that of the nanoslit (see Fig. S2).

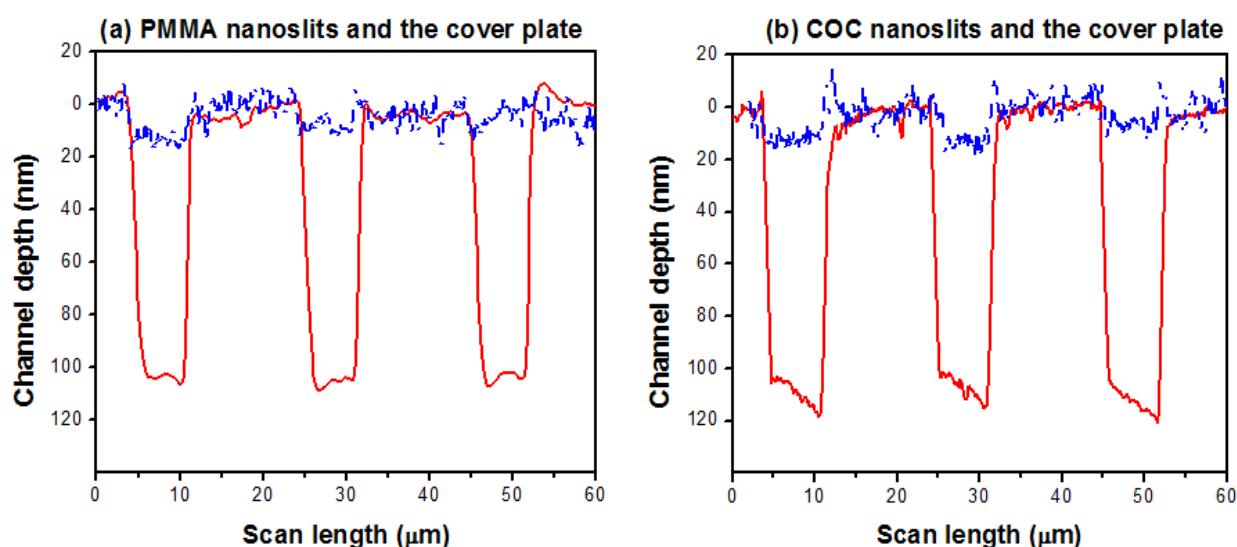


Fig. S2. AFM profiles measured for (a) PMMA and (b) COC nanoslits and their respective cover plates after invoking the appropriate assembly protocol, which entailed thermal fusion bonding at 87°C for PMMA and 115°C for COC. The solid-red traces are the profiles of the nanoslits and the dashed-blue traces are profiles of the cover plates. In both cases, the cover plate was carefully peeled from the substrate following the thermal fusion bonding process and then, subjected to AFM.

XPS surface analysis

Following oxygen plasma treatment of the polymeric material, the O1s/C1s ratio of PMMA and COC surfaces increased as shown in Table S1. These results confirmed the introduction of oxygen-containing functional groups onto the PMMA (Fig. S3a) and COC (Fig. S3b) surfaces as discerned from the XPS data.¹ In the accompanying figures (Fig. S3), the survey spectra of the oxygen plasma treated surfaces were shifted both in the X and Y direction for clarity.

Table S1. XPS O1s/C1s data for PMMA and COC.

Sample	O1s/C1s
PMMA-Native	0.279
PMMA-O ₂ plasma	0.357
COC-Native	0.0650
COC-O ₂ plasma	0.182

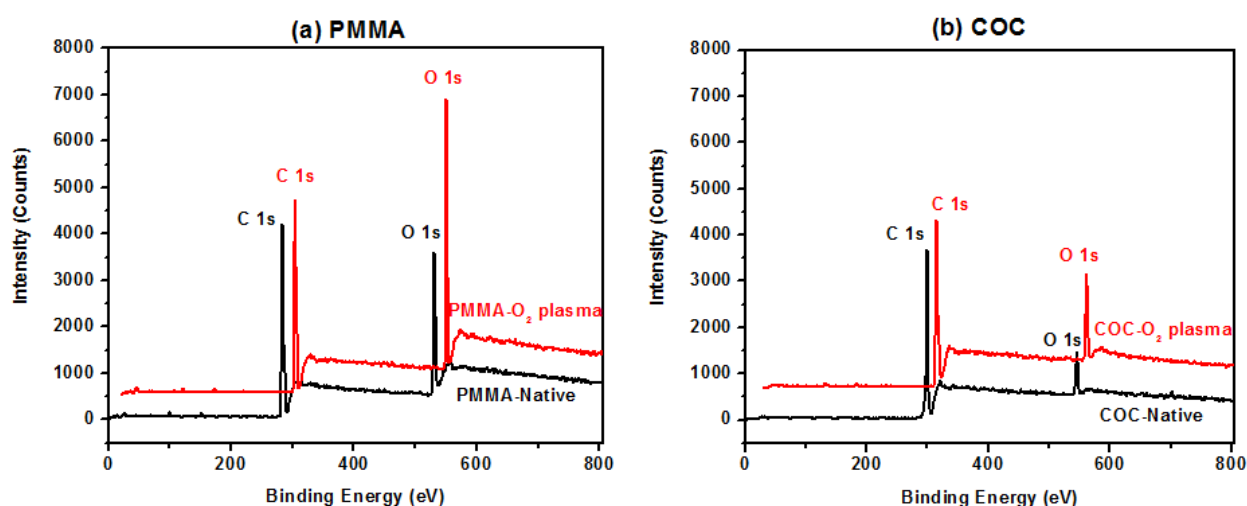


Fig. S3. XPS survey spectra of (a) PMMA and (b) COC, before (black trace) and after (red trace) oxygen plasma treatment. XPS conditions consisted of an AlK α source and a hemispherical electron energy analyzer.² The pressure in the analyzing chamber was $<3 \times 10^{-9}$ Torr with an 80 eV pass energy and 150 W X-ray beam for recording the survey spectra.

Intermittent movement of dsDNA molecules in polymer nanoslits

Intermittent electrophoretic movements of dsDNA in COC nanoslits were monitored to determine if these polymer nanoslits functioned similar to fused silica devices.³ Fig. S4a presents micrographs of the intermittent movement in COC nanoslits; frame #2 shows the DNA beginning to pause inside the nanoslit and after frame #5, it finally moved into the microchannels (see frame #6). Similar observations have been reported by Salieb-Beugelaar *et al.* for nanoslits

fabricated in fused silica (20 nm deep, 3 μm wide), which produced a field dependent mobility.³

Fig. S4b shows complete cessation of movement of two λ -DNA molecules inside COC nanoslits taken from frames #1, #5, and #10.

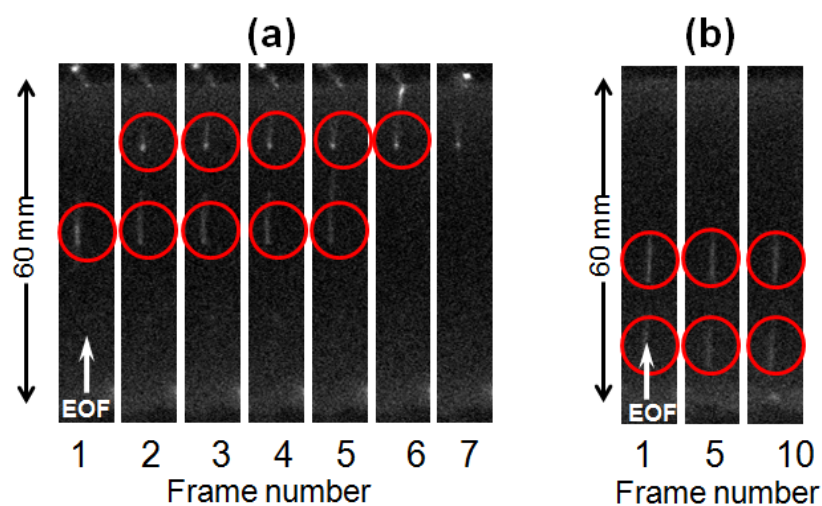


Fig. S4. Fluorescence images of λ -DNA stained with YOYO-1[®] showing (a) intermittent movement and (b) no movement occurring inside COC nanoslits while applying a field strength of 126 V/cm. The frame rate used was 20 frames per second. The λ -DNA-YOYO-1[®] complexes (250 ng/mL) were seeded into a running buffer consisting of 40 mM TAE, pH 8.30, and β -mercaptoethanol (4% v/v) to minimize photobleaching artifacts.

References

1. J. Chai, F. Lu, B. Li and D. Y. Kwok, *Langmuir*, 2004, **20**, 10919-10927.
2. S. Balamurugan, A. Obubuafo, S. A. Soper, R. L. McCarley and D. A. Spivak, *Langmuir*, 2006, **22**, 6446-6453.
3. G. B. Salieb-Beugelaar, J. Teapal, J. van Nieuwkastele, D. Wijnperle, J. O. Tegenfeldt, F. Lisdat, A. van den Berg and J. C. T. Eijkel, *Nano Lett.*, 2008, **8**, 1785-1790.